

# Chemical Environment of Copper Aggregates Embedded in Polypyrrole Films: The Nature of the Copper–Polypyrrole Interaction

N. Watanabe,<sup>†,‡</sup> J. Morais,<sup>§</sup> and M.C. Martins Alves<sup>\*,†</sup>

Laboratório Nacional de Luz Síncrotron, P.O. Box 6192, 13084–971, Campinas, Brazil, Instituto de Química, UNICAMP, P.O. Box 6154, 13083-970, Campinas, Brazil, and Instituto de Física, Universidade Federal do Rio Grande do Sul, Av. Bento Gonçalves, 9500, 91501–970, Porto Alegre, Brazil

Received: October 25, 2001; In Final Form: March 14, 2002

We report on the structural and electronic properties of copper aggregates embedded in composite polypyrrole films studied by X-ray absorption techniques (XAS). Measurements at the Cu K edge during in situ reduction suggest that the reaction starts with the formation of the complex  $[-[(C_4H_2N)_3CH_3(CH_2)_{11}OSO_3^-]_yCu^{2+}]_n$  ( $y = 4$ ), in which the copper is bonded to oxygen atoms. The reduction of this complex leads to the synthesis of Cu metal aggregates in the film. Measurements at the N K edge evidence that the incorporation of the metal in the polymer network does not disturb the electronic structure nor the environment of the nitrogen from the pyrrole unit. Measurements at the O K edge indicate that the metal/polymer interaction happens via hybridization of O 2p and Cu 3d orbitals, resulting in an enlace that has a quasi-covalent character. Scanning electron microscopy measurements show that dendritic-like copper aggregates are formed on the film surface.

## Introduction

Composite materials consisting of metal aggregates and conducting polymers attract considerable interest for basic research because of their technological applications in heterogeneous catalysis,<sup>1</sup> environmental science,<sup>2</sup> microelectronics,<sup>3</sup> and magnetism.<sup>4</sup>

One way to prepare these materials is by the electrochemical method that has the advantages of low cost and simplicity. In this process, the composite material is synthesized by the oxidation of the respective monomer and further deposition of the metallic species from an aqueous solution of the suited cation. By monitoring the deposition time, the loading and the size of the metal aggregates is controlled. This method has been applied to produce a wide range of composites such as Cu aggregates on polythiophene,<sup>1b,1d</sup> or Pt, Cu, and Ni aggregates on polypyrrole (PPy),<sup>1g,1h</sup> as well as Au aggregates in polyaniline (PANI).<sup>5</sup>

To explore the possibility of practical applications of such composites in magnetic recording devices,<sup>4</sup> we have prepared granular systems adopting the same methodology used to obtain electrocatalysts.<sup>1b,d,15</sup> The present investigation is about the deposition of copper on PPy aiming future studies on magnetic Cu alloys containing a ferromagnetic metal such as Fe, Co, and Ni.

The performance of metal/polymer composites as magnetic devices is strongly dependent on the chemical interaction between the metal and the polymer<sup>6</sup> as well as the metal crystalline structure<sup>7</sup> and the chemical bond at the surface. Nevertheless, there is still very limited knowledge at the microscopic level concerning the factors which determine the structure and consequently the electronic and chemical properties

of these systems. This has stimulated many studies regarding, for instance, the ion dynamics during the redox process<sup>1g,9</sup> or spectroscopic studies using IR–UV–vis,<sup>5</sup> XPS (X-ray photoelectron spectroscopy),<sup>5,10,11</sup> Raman,<sup>10,11</sup> NMR,<sup>12</sup> or diffraction techniques.<sup>11</sup>

Some reports on polypyrrole (PPy)/Cu composites ascertain the formation of a Cu(I)–PPy complex where the copper is bonded to the nitrogen from the pyrrolic unit.<sup>11</sup> A nitrogen-stabilized Cu(I)–N complex present at least on the surface of the copper composites observed by XPS and cyclic voltammetry was also reported.<sup>10</sup> A Cu–O interaction was proposed for copper in polythiophene.<sup>1b,1d</sup> The formation of complexes in Au(I)–PPy and Au(III)–PPy<sup>12</sup> composites was also suggested. In the case of Au/PANI, it was stated that the metal/polymer interaction takes place at the nitrogen linkages.<sup>5</sup>

We propose another approach to investigate the interaction between the polymer and the metal aggregates by directly probing the evolution of the unoccupied states in the metal and in the polymer by using the XAS (X-ray absorption spectroscopy) technique. This kind of study gives a more complete understanding of the metal/polymer interface. XAS is a powerful technique to probe the electronic and structural properties of a selected atom in a matrix.<sup>13</sup> In addition, XAS allows us to investigate the effect of charge transfer<sup>14</sup> processes in the electronic structure of the composite elements.

In this paper, we describe a systematic study on the formation of the Cu/PPy composite. In situ XAS measurements at the Cu K edge allowed us to track the electrochemical incorporation of Cu<sup>2+</sup> in the PPy/SDS films and to follow the reduction of Cu<sup>2+</sup> to Cu<sup>0</sup>. The quantitative parameters obtained from EXAFS (extended X-ray absorption fine structure; number of neighbors, distances, and disorder) allowed us to propose a model for the complex formed at the initial stages of the process and to determine the compositional and structural evolution of the Cu aggregates at all stages of the electrochemical process. In addition, we have verified the influence of the metal in the electronic properties of the polymer by measuring the XANES

\* To whom correspondence should be addressed. Phone: 55 19 32874520. Fax: 55 19 32874632. E-mail: maria@lnls.br.

<sup>†</sup> Laboratório Nacional de Luz Síncrotron.

<sup>‡</sup> Instituto de Química, UNICAMP.

<sup>§</sup> Universidade Federal do Rio Grande do Sul.

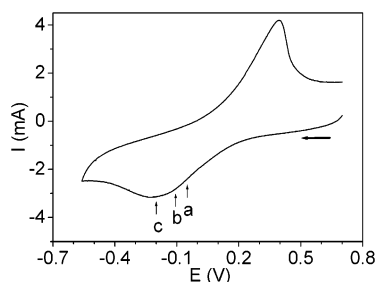


**Figure 1.** Cyclic voltammetry curve of PPy-SDS film deposited on glassy carbon immersed in 0.01 M  $\text{CuSO}_4\text{-H}_2\text{SO}_4$  0.1 M, scan rate = 20 mV/s. Arrows indicate the potentials at which the XAS spectra were acquired: stage a,  $-0.05$  V; stage b,  $-0.10$  V; and stage c,  $-0.20$  V.

(X-ray absorption near edge spectroscopy) spectra at the N and O K edges for the PPy/SDS films containing the copper aggregates. SEM measurements were used to obtain the morphology of the final material.

## Experimental Section

**Chemicals.** Samples were electrochemically produced with a solution composed of  $\text{CuSO}_4$  0.01 M (Puratronic 99.999%), SDS- $(\text{CH}_3(\text{CH}_2)_{11}\text{OSO}_3^-\text{Na}^+)$  0.01 M (Mallinckrodt, 95%),  $\text{H}_2\text{SO}_4$  0.1 M (Carlo Erba, 96%), and pyrrole 0.02 M (Alfa Aesar, 98%, purified by distillation just before use). Solutions were prepared using Millipore Milli-Q deionized water. The final pH was 1.4.

**Electrochemical Experiments.** All of the electrochemical measurements were performed at room temperature using an EG&G PAR model 273A potentiostat/galvanostat interfaced with a PC. The working electrode was a glassy carbon disk (Goodfellow 99.99%,  $\phi = 10$  mm, 2 mm thick). A Pt wire was used as a counter electrode, and all potentials were referred to the Ag/AgCl electrode. Prior to any measurement, the glassy carbon electrode was polished with  $0.3\ \mu\text{m}$  alumina suspension on a microcloth polishing pad and rinsed with deionized water in an ultrasonic bath.

**Preparation of (PPy)/SDS-Cu Films.** Polypyrrole films were grown on glassy carbon disks by applying  $+0.9$  V (vs Ag/AgCl) during 600 s, producing polypyrrole films approximately  $0.4\ \mu\text{m}$  thick. The copper deposition was done at three different potentials:  $-0.05$ ,  $-0.10$ , and  $-0.20$  V (vs Ag/AgCl). These potentials were chosen based on the cyclic voltammetric response of the system (Figure 1). These potentials were applied during 600 s in order to attain the equilibrium of the system, and then XAS measurements were performed, keeping the potential control.

**XAS Measurements.** In situ XAS measurements at the copper K edge were performed at the Laboratório Nacional de Luz Síncrotron, LNLS, using the XAS beam line.<sup>16</sup> A "channel cut" Si (111) crystal monochromatized the collimated X-ray beam. Vertical slits of 0.5 mm placed before the monochromator provided an energy resolution of 2.7 eV. The monochromator was calibrated at the Cu K edge using a Cu metal foil.

In our experiments, we used a thin-layer electrochemical cell,<sup>17</sup> developed at LNLS. The cell was mounted on a goniometer stage, and the incident beam formed an angle of  $10^\circ$  with respect to the substrate surface. The intensity of the incoming X-ray beam was measured using an ionization chamber. A NaI scintillator placed on the top of the electrochemical cell measured the fluorescence photons emitted by the sample.

EXAFS spectra were recorded from 8900 to 9500 eV with a 2.0 eV step and an acquisition time of 2 s/point. Five scans

were averaged to obtain a good signal-to-noise ratio. The XANES spectra were recorded from 8940 to 9160 eV with 0.8 eV steps and 2 s/point.

The WINXAS program<sup>18</sup> was used for data analysis. A linear preedge background was subtracted, and the spectra were normalized to the height of the absorption edge. The EXAFS signal between 2.5 and  $11\ \text{\AA}^{-1}$  was Fourier transformed with a  $k^2$  weighting and a Kaiser window. Structural parameters were obtained from least-squares fitting in the  $R$  space using theoretical phase shift and amplitude functions deduced from the FEFF6 code.<sup>19</sup> The energy shifts,  $\Delta E_0$ , were obtained by analyzing the first shell of the reference spectra of bulk CuO and Cu metal,  $\Delta E_0(\text{CuO}) = -6$  eV and  $\Delta E_0(\text{Cu-Cu}) = 2.4$  eV. The analysis was done by keeping  $\Delta E_0$  fixed to the reference values. In the fitting procedure, the number of free parameters did not exceed the number of independent data points given by the Nyquist theorem.<sup>20</sup>

XANES measurements at the O and N K edges were performed at the SGM (spherical grating monochromator) beam line at LNLS. The resolving power ( $E/\Delta E$ ) of the spherical grating is better than 3000. The spectra were collected in the total electron-yield mode by measuring the sample current. The spectra were normalized to the photon flux using the yield of a gold mesh, 95% transparent, placed 15 cm upstream from the sample. Photon beam dimensions were about  $1 \times 1$  mm at the sample and normal incidence was used.

**SEM Measurements.** The morphology of the films was observed using a low vacuum microscope JSM5900F-LME/LNLS.

## Results

**Electrochemistry.** The doping mechanism of polypyrrole films has been described previously.<sup>1h</sup> When the monomer is oxidized in the presence of a surfactant, such as SDS, the anion of the surfactant is irreversibly incorporated into the structure of the polymer. When this film is negatively polarized in the presence of cations, it behaves as cation-exchange membrane; that is, the negative charge created in the polymer network is neutralized by the incorporation of cations from the solution.

The voltammetric response, of PPy/SDS film deposited on glassy carbon in the presence of  $\text{Cu}^{2+}$  ions, displays one cathodic peak at  $-0.20$  V and one anodic peak at  $0.37$  V (vs Ag/AgCl; Figure 1). The cathodic peak corresponds to the up-take and reduction of  $\text{Cu}^{2+}$  to  $\text{Cu}^0$  in the PPy/SDS film, and the anodic peak corresponds to the dissolution of  $\text{Cu}^0$  aggregates.

The in situ Cu K edge XAS measurements were acquired at different potentials (or stages) based on the voltammetric response of the PPy/SDS film. The spectra were taken in the beginning of the process, at  $-0.05$  V (stage a), and at more reductive potentials at  $-0.10$  (stage b) and  $-0.20$  V (stage c). The potential of each stage was controlled during the XAS measurements thus avoiding any oxidation of the film during the measurements.

**EXAFS at the Cu K Edge.** The in situ Cu K edge EXAFS spectra obtained at stages a, b, and c are displayed in Figure 2 with reference compounds ( $\text{CuSO}_4$  and Cu metal) for comparison.

The EXAFS spectrum of  $\text{CuSO}_4$  has a sharp edge (feature A) that corresponds to the transition of one photoelectron from the 1s to the 4p level.<sup>21</sup> The smooth oscillations (B and C) that appear after the edge are related to the oxygen environment around copper.<sup>21</sup> For Cu metal, the transition from the 1s level appears at lower energy (A'), and the photoelectron is ejected to hybridized p-d states.<sup>22</sup> The shape of the oscillations after

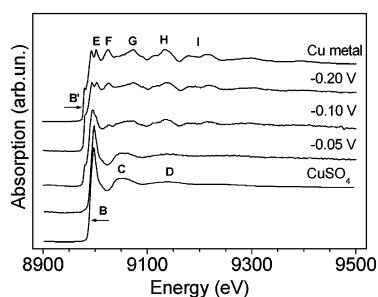


**Figure 2.** In situ EXAFS spectra obtained at the Cu K edge as a function of the applied potential in comparison with the spectra of CuSO<sub>4</sub> and Cu metal references.

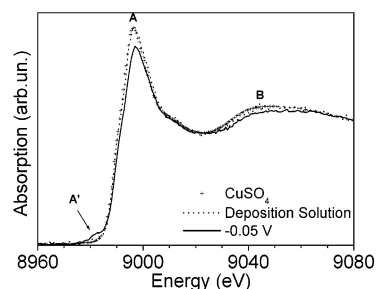


**Figure 3.** Comparison of the in situ XANES spectra obtained for the CuSO<sub>4</sub>, for the deposition solution (CuSO<sub>4</sub>, SDS, and H<sub>2</sub>SO<sub>4</sub>) and at -0.05 V (stage a).

the edge (D, E, F, G, and H) is characteristic of copper in a face-centered cubic (FCC) packing.

The following changes are observed for the different stages. At -0.05 V (stage a), the spectrum is quite similar to that of CuSO<sub>4</sub>. At -0.10 V (stage b), the raising of a preedge feature (A'), followed by the decrease in intensity of the main edge (A) and the appearance of features D, E, F, G, and H, indicates the initial Cu reduction (Cu<sup>2+</sup> → Cu<sup>0</sup>) in the PPy/SDS film. At -0.20 V (stage c), the spectrum is identical to that of Cu metal.

**XANES at the Cu K Edge.** To verify if some interaction took place inside the solution prior to the copper deposition, we have compared the XANES spectra of the pure CuSO<sub>4</sub> with that of the deposition solution (CuSO<sub>4</sub> + SDS + Py monomer) and of the film obtained at -0.05 V (stage a; Figure 3). The spectra of pure CuSO<sub>4</sub> and the deposition solution are practically identical showing no significant change in the close environment of Cu<sup>2+</sup> species and that the complexation does not occur in solution. The spectrum obtained at -0.05 V (stage a) presents changes in the intensities of the preedge feature (A') and main edge. These changes indicate that the Cu<sup>2+</sup> species are in a distorted<sup>23,24</sup> and more disordered site in the PPy/SDS film. These results clearly show the formation of the Cu-SDS complex in the film.

The XAS results allow us to give a more complete description of the copper species present in the PPy/SDS film. Initially (at -0.05 V, stage a), the electrochemical reaction starts with the reduction of the PPy/SDS film with concomitant incorporation of cations, Cu<sup>2+</sup>, from the solution. The Cu<sup>2+</sup> species are surrounded by oxygen atoms from the surfactant, (OSO<sub>3</sub><sup>-</sup>), anion dopant trapped in the film. At a more negative potential (-0.10 V, stage b), a partial reduction of the Cu<sup>2+</sup> ions to Cu<sup>0</sup> occurs, so both species coexist in the film. At -0.20 V (stage c), all the copper present in the PPy/SDS film is in the completely reduced form Cu<sup>0</sup>.

The spectrum for the PPy/SDS film obtained at the -0.10 V (stage b) was deconvoluted considering the contribution of Cu<sup>2+</sup> and Cu<sup>0</sup> species. A linear combination of the XANES spectra

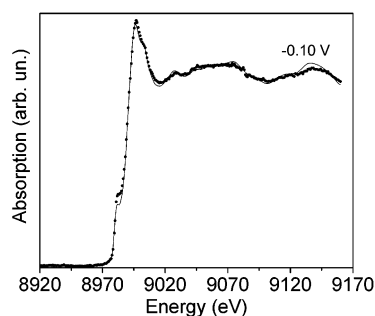


**Figure 4.** Best fit obtained for the linear combination of the XANES spectra for the film obtained at -0.10 V (stage b) considering the contribution of 37 ± 5% of Cu<sup>2+</sup> and 63 ± 5% of Cu<sup>0</sup> (dots, experimental points; line, fitting).

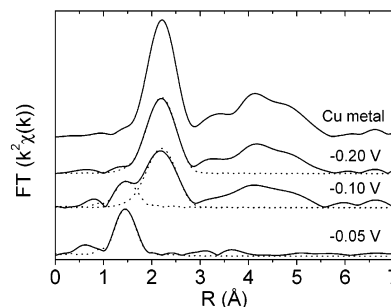


**Figure 5.** Fourier Transform of the EXAFS signal at the Cu K edge as a function of the applied potential. The dash-dotted lines correspond to the fitting result. At -0.05 V, a Cu-O pair was taken into account. At -0.10 V, two distances were fitted: Cu-O and Cu-Cu. At -0.20 V, the fit was performed with the Cu-Cu pair.

**TABLE 1: Results Obtained from the Quantitative Analysis of the Coordination Shell Yielding the Coordination Number (*N*), Distance (*R*), and the Debye Waller Factor (*σ*)**

stage	type of neighbor	<i>N</i>	<i>R</i> (Å)	<i>σ</i> <sup>2</sup> (Å <sup>2</sup> )
-0.05 V	O	4 ± 0.5	1.93 ± 0.01	0.0013 ± 0.00026
-0.10 V	O	2 ± 0.5	1.99 ± 0.01	0.017 ± 0.00024
	Cu	7 ± 0.5	2.56 ± 0.01	0.0098 ± 0.0024
-0.20 V	Cu	12 ± 0.5	2.56 ± 0.01	0.0096 ± 0.0019
Cu metal	Cu	12	2.56	0.0080

of CuSO<sub>4</sub> and Cu metal was performed, and the best simulation result is shown in Figure 4. These results show that 37 ± 5% of the copper in the film is in the Cu<sup>2+</sup> state and 63 ± 5% in the Cu<sup>0</sup> state. As these measurements were performed in the presence of electrolyte with Cu<sup>2+</sup>, we have measured the contribution of the solution alone, and it accounts for 15% of the Cu<sup>2+</sup> signal, so we conclude that the remaining 22% of Cu<sup>2+</sup> ions are incorporated into the PPy/SDS film.

The Fourier transform (FT) of the EXAFS oscillations (Figure 5) reflects the average radial distribution function around Cu atoms in the PPy/SDS film. The changes in the FT confirm the evolution shown by the raw EXAFS spectra. At -0.05 V (stage a), the peak at about 1.5 Å, corresponds to oxygen neighbors. At more reductive potentials, copper atoms gradually replace the atoms in the oxygen shell. At -0.20 V (stage c), only Cu-Cu distances are observed. The presence of next-nearest neighbors in the FT (peaks at 3.3, 4.1, and 4.7 Å) indicate the formation of bulk copper with medium-range order organization of the atomic shells.

The resulting quantitative analysis of the first shell in the FT is presented in Table 1.

At -0.05 V (stage a), the coordination shell corresponds within the uncertainty to four *N* = 4 ± 0.5 oxygen atoms at an average distance of *R* = 1.93 ± 0.01 Å with small mean-square



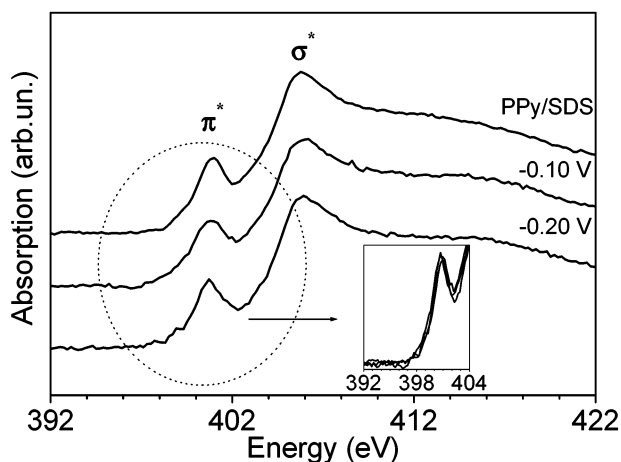


**Figure 6.** XANES spectra at the N K edge for the PPY/SDS films obtained at  $-0.10$  (stage b) and  $-0.20$  V (stage c) in comparison with a pure PPY/SDS film. The inset shows the superposition of the preedge regions.

relative displacement. The distance found is between the Cu–O bond length in  $\text{CuSO}_4$  ( $N = 4$ ,  $R = 1.88$  Å) and  $\text{CuO}$  ( $N = 4$ ,  $R = 1.96$  Å) and shorter than the one found by Tourillon et al.<sup>1b,1d</sup> for the Cu–O bond ( $R = 1.91$  Å) for copper in polythiophene. At this stage, we assign the formation of  $\text{Cu}^{2+}(\text{OSO}_3^-)_4$  links in the PPY/SDS film.

At  $-0.10$  V (stage b), the two distances at  $R = 1.99 \pm 0.01$  and  $2.54 \pm 0.01$  Å correspond to copper atoms in both the oxidized and metallic form. The coordination numbers obtained  $N = 2 \pm 0.5$  and  $7 \pm 0.5$  are lower than the bulk values expected for  $\text{CuO}$  and  $\text{Cu}$  metal. The Debye Waller factors are very high,  $\sigma^2 = 0.017 \pm 0.00024$  and  $0.098 \pm 0.0024$ , indicating that the oxide and the metal structures have high structural disorder.

At  $-0.20$  V (stage c), the distance of  $R = 2.56 \pm 0.01$  Å and the coordination number of  $N = 12 \pm 0.5$  indicate the complete reduction of  $\text{Cu}^{2+}$  and formation of bulk copper. The Debye Waller factor is larger than that one found for the metal foil suggesting the presence of a more disordered first shell for the Cu aggregates.

We have also performed the fitting for the Cu–Cu distances beyond the coordination shell, and even for the film polarized at  $-0.10$  V, the bulk Cu metal values were obtained.

After the measurements performed at the Cu K edge, the PPY/SDS films at selected stages and a pure PPY/SDS film were transferred to a UHV chamber in order to perform the corresponding XAS measurements at the N and O K edges.

**XANES at the N and O K Edges.** XANES spectra of organic molecules are dominated by transitions:  $\pi^*$  and  $\sigma^*$ .<sup>25</sup> The  $\pi^*$  are sharp structures that correspond to the transition of a  $1s$  photoelectron into an empty or partially filled antibonding  $2p\pi^*$  orbital. The  $\sigma^*$  are broad resonances interpreted as arising from backscattering of the photoelectrons ejected at low kinetic energy by atoms adjacent to the absorbing atom<sup>26</sup> or as a temporary trapping of the ejected photoelectrons by a centrifugal molecular potential barrier.<sup>27</sup>

The N K edge XANES of the PPY/SDS film (Figure 6) has one intense  $1s \rightarrow 2p\pi^*$  resonance (at 401 eV) and one  $\sigma^*$  resonance (407 eV). These assignments are in agreement with the findings of Pavlychev et al.<sup>28</sup> The comparison of the spectra from the films with Cu aggregates and the pure polymer shows that there is no significant difference between them (Figure 5, see inset). This indicates that the incorporation of copper into the polymer matrix does not affect the electronic structure and the environment of the N from the pyrrole unit.

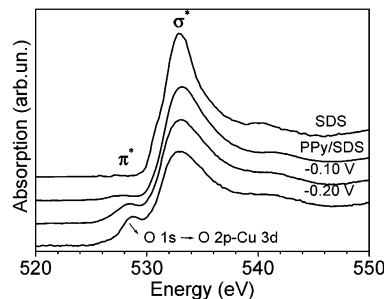


**Figure 7.** XANES spectra at the O K edge for the PPY/SDS films obtained at  $-0.10$  (stage b) and  $-0.20$  V (stage c) in comparison with a PPY/SDS film and pure SDS.

The O K edge XANES of pure SDS (Figure 7) has a very weak  $\pi^*$  resonance (at 527 eV) and one  $\sigma^*$  resonance (at 533 eV). The spectrum of the PPY/SDS film is quite similar to the one of pure SDS, with small changes in the intensity and width of features which are associated to structural disorder. The resemblance of this signal with that of pure SDS shows that the oxygen species present in the PPY/SDS film are from the  $\text{OSO}_3^-$  anion dopant provenient from the surfactant.

The spectra of the films with Cu aggregates show the gradual appearance of a preedge feature at 528 eV. This feature becomes narrower and more intense for the film polarized at  $-0.20$  V (stage c). The position of the  $\sigma^*$  resonance remains at the same position for all samples.

The XANES spectra at the O K edge for transition metal oxides and chemisorbed oxygen on copper and nickel<sup>29</sup> display a sharp edge assigned to the  $1s$  transition to hybridized states of predominantly metal  $3d$  character with O  $2p$  contribution. This feature should not appear in a pure ionic compound because an  $\text{O}^{2-}$  ion has no unoccupied  $2p$  states and the  $1s \rightarrow 2p$  contribution to the spectrum would be missing for purely ionic oxides. The strength of the  $1s \rightarrow 2p$  channel increases with increasing covalency of the bond.<sup>29</sup>

The preedge feature that appears for PPY/SDS films with copper aggregates may be assigned to the creation of new empty states after the formation of a bond between copper and the  $\text{OSO}_3^-$  anion dopant trapped in the film. The covalence of this bond increases with the increase of the copper content, i.e., going from  $-0.10$  to  $-0.20$  V. No modification in the bond length is expected since the  $\sigma^*$  resonance remained at the same position.<sup>26</sup>

**SEM Measurements.** A scanning-microscope observation of the PPY/SDS film obtained at  $-0.20$  V (stage c) reveals the formation of dendritic copper grown on the surface of the film (Figure 8). Each dendrite has various branches with sizes in the range of few micrometers.

## Discussion and Conclusions

The electrochemical synthesis of polypyrrole involves three pyrrole units per counterion.<sup>30</sup> The XAS results at the Cu K edge showed the formation of a Cu–O bond at the initial stage of the process. The quantitative analysis yielded for the coordination shell four ( $4 \pm 0.5$ ) oxygen atoms at  $1.93 \pm 0.01$  Å. The distance and coordination number values are close to those for copper oxide ( $\text{CuO}$ ) ( $N = 4$ ,  $R = 1.96$  Å), where four oxygen atoms are in a nearly square planar configuration to form  $\text{CuO}_4$  units.<sup>31</sup> Excluding the possibility of the formation of a  $\text{Cu(II)}\text{--SDS}$  complex in solution, we propose a model for the complex formed at the initial stages of the process based on the above results, as shown in Figure 9.

At more reductive potentials, the  $\text{Cu}^{2+}$  ions from the solution are discharged on the copper initially bonded in the polymer

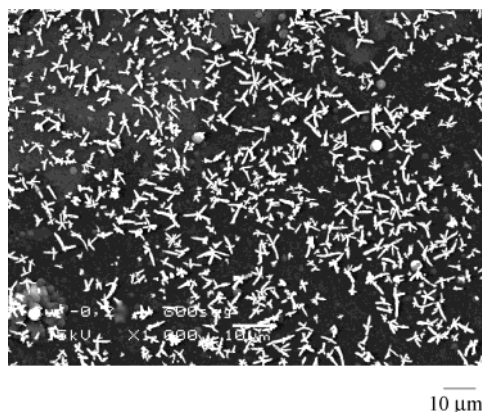


**Figure 8.** SEM image taken for the PPy/SDS-Cu film obtained at  $-0.20$  V (stage c).

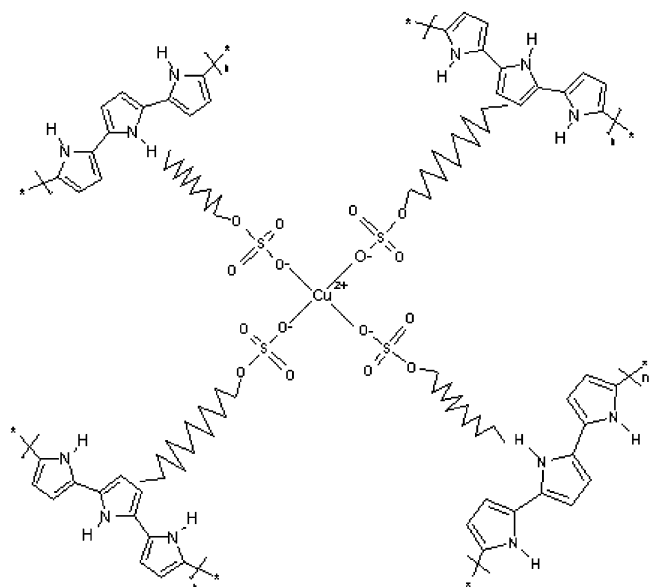


**Figure 9.** Schematic drawing of the proposed Cu complex formed in the initial stages of the electrochemical process. The zigzag lines represent the  $-\text{CH}_3(\text{CH}_2)_{11}-$  radical.

network. According to this model, the doped part of the polymer would be able to bind the copper species.

The XAS measurements at the N K edge showed that the N environment from the pyrrole is not disturbed by the presence of copper in the polymer matrix. The O K edge evidenced the hybridization of O 2p and Cu 3d orbitals, resulting in a quasi-covalent enlace for Cu and O from the  $\text{OSO}_3^-$  anion. The formation of this bond would explain the chemical stability of such  $\text{Cu}^0/\text{PPy}/\text{SDS}$  composites.

It is important to point out that the XAS technique enables one to track the evolution of the unoccupied density of states induced by charge-transfer processes. So, any change in the  $\pi^*$  region of the polymer would indicate some interaction between the metal and the polymer.<sup>32</sup> Our XAS results demonstrated these changes only at the O-K edge.

Other authors have proposed the formation of a chemical bonding between copper and the nitrogen from the pyrrolic unit;<sup>10,11</sup> however, in their case, the Cu-PPy composites were deposited under synthesis conditions markedly different. Moreover, we have observed that the pH of the solution influences the protonation of the nitrogen from the pyrrolic unit. In this study, the pH of the deposition solution is 1.4; at this condition, the nitrogen from the pyrrole is protonated thus avoiding any possibility of interaction with the metal.

Additional XAS calculations taking into account the interaction between the polymer and the metal are under way. Other measurements concerning the study of the valence band of these materials and depth profiling of the metal aggregates are being planned.

In conclusion, we have characterized the electronic and structural properties of Cu aggregates in PPy/SDS films. EXAFS measurements at the Cu K edge evidenced the formation of a complex between Cu and the  $\text{OSO}_3^-$  anion at the initial stages of the process. This complex is subsequently reduced to Cu metal at more negative potentials. The main interaction between Cu aggregates and the polymer is verified via Cu-O bonds. SEM measurements shows dendritic-like copper being formed on the PPy/SDS film surface.

**Acknowledgment.** We thank Miguel Abbate, Sérgio R. Teixeira, and Aline Y. Ramos for fruitful discussions and suggestions. We are indebted to the staff of LNLS for operating the storage ring and the assistance during the experiments at the XAS and SGM beamlines. The beam time was supported by LNLS under the proposals XAS 581/99 and SGM 689/00. Thanks are also addressed to Daniel Ugarte and Paulo C. Silva for their help during the SEM measurements. This work was partially supported by the Brazilian Funding Agencies FAPESP (Proc. No. 99/07872-4, 97/06967-6, and 95/06439-4) and Pronex. N.W. thanks the CNPq (Proc.144894/98-0) for her Ph.D. fellowship. We also thank Diane M. Petty for the revision of the English of this manuscript.

## References and Notes

- (1) (a) Kost, K. M.; Bartak, D. E.; Kazee, M.; Kuwana, T. *Anal. Chem.* **1988**, *60*, 2379. (b) Tourillon, G.; Dartyge, E.; Dexpert, H.; Fontaine, A.; Jucha, A.; Lagarde P.; Sayers, D. E. *J. Electroanal. Chem.* **1984**, *178*, 357. (c) Laborde, H.; Léger, J.-M.; Lamy, C. *J. Appl. Electrochem.* **1994**, *24*, 1019. (d) Tourillon, G.; Dartyge, E.; Fontaine, A.; Jucha, A. *Phys. Rev. Lett.* **1986**, *57*(5), 603. (e) Lee, J. Y.; Tan, T.-C. *J. Electrochem. Soc.* **1990**, *137*(5), 1402. (f) Deronzier, A.; Moutet, J.-C. *Coord. Chem. Rev.* **1996**, *147*, 339. (g) Hepel, M. *J. Electrochem. Soc.* **1998**, *145* (1), 124. (h) Hepel, M.; Chen, Y. M.; Stephenson, R. *J. Electrochem. Soc.* **1996**, *143*(2), 498.
- (2) Hepel, M.; Dentrone, L. *Electroanalysis* **1996**, *8* (11), 996.
- (3) White, H. S.; Kittlesen, G. P.; Wrighton, M. S. *J. Am. Chem. Soc.* **1984**, *106*, 5375.
- (4) Langlais, V.; Arri, S.; Pontonnier, L.; Tourillon, G. *Scripta Mater.* **2001**, *44*, 1315.
- (5) Hatchett, D. W.; Josowicz, J.; Janata, J.; Baer, D. R. *Chem. Mater.* **1999**, *11*, 289.
- (6) Ernst, F. *Mater. Sci. Eng.* **1995**, *R14*, 97.
- (7) Respaud, M.; Broto, J. M.; Rakoto, H.; Fert, R.; Thomas, L.; Barbara, B.; Verelst, M.; Snoeck, E.; Lecante, P.; Mosset, A.; Osuna, J.; Ould-Ely, T.; Amiens, C.; Chaudret, B. *PRB* **1998**, *57*(5), 2925.
- (8) Peres, R. C. D.; De Paoli, M. A.; Torresi, R. M. *Synth. Met.* **1992**, *48*, 259.
- (9) Maia, G.; Torresi, R. M.; Ticianelli, E. A.; Nart, F. C. *J. Phys. Chem.* **1996**, *100*, 15910.
- (10) Cioffi, N.; Torsi, L.; Losito, I.; Di Franco, C.; De Bari, I.; Chiavarone, L.; Scamarcio, G.; Tsakova, V.; Sabbatini, L.; Zamboni, G. *J. Mater. Chem.* **2001**, *11*, 1434.
- (11) Liu, Y. C.; Hwang, B. J. *Thin Solid Films* **1999**, *339*, 233.
- (12) Rau, J.-R.; Lee, J.-C.; Chen, S.-C. *Synth. Met.* **1996**, *79*, 69. (b) Rau, J.-R.; Chen, S.-C.; Tang, H.-Y. *Synth. Met.* **1997**, *90*, 115.
- (13) Koningsberger, D. C.; Prins, R. X-ray Absorption: Principles, applications and techniques of EXAFS, SEXAFS and XANES. In *Chemical Analysis*; John Wiley & Sons: New York, 1988; Vol. 92.
- (14) Alves, M. C. M.; Dodelet, J. P.; Guay, D.; Ladouceur, M.; Tourillon, G. *J. Phys. Chem.* **1992**, *96*(26), 10898. (b) Alves, M. C. M.; Tourillon, G. *J. Phys. Chem.* **1996**, *100*(18), 7566.
- (15) Pitchaimani, S.; Pattabiraman, R. *Bull. Electrochem.* **1999**, *15*(11), 433.
- (16) Tolentino, H.; Cezar, J. C.; Cruz, D. Z.; Compagnon-Caillol, V.; Tamura, E.; Alves, M. C. M. *J. Synchrotron Rad.* **1998**, *5*, 521.
- (17) Sharpe, L. R. *Chem. Rev.* **1990**, *90*, 705. (b) Tadjeddine, A.; Tourillon, G.; Guay, D. *Electrochim. Acta* **1991**, *36*(11-12), 1859.
- (18) Ressler, T. *J. Phys. IV France* **1997**, *7*, C2-269.

- (19) Rehr, J. J.; Mustre de Leon, J.; Zabinsky, S. I.; Albers, R. C. *J. Am. Chem. Soc.* **1991**, *113*, 5135.
- (20) Lytle, F. W.; Sayers, D. E.; Stern, E. A. *Physica B* **1989**, *158*(1–3), 701.
- (21) Briois, V.; Cartier, C.; Momenteau, M.; Maillard, P.; Zarembovich, J.; Dartyge, E.; Fontaine, A.; Tourillon, G.; Thuery, P.; Verdaguer, M. *J. Chim. Phys. Biol.* **1989**, *86*(7–8), 1623.
- (22) Pizzini, S.; Baudalet, F.; Fontaine, A.; Chandresis, D.; Magnan, H.; Fert, A.; Marliere, C. *Appl. Surf. Sci.* **1993**, *69*(1–4), 7.
- (23) Petiau, J.; Calas, G.; Saintavit, P. *J. Phys. Paris* **1987**, *48* (C-9), 1085.
- (24) Galois, L.; Calas, G.; Arrio, M. A. *Chem. Geol.* **2001**, *174*, 301.
- (25) Stohr, J.; Jaeger, J. *Phys. Rev. B* **1982**, *26*, 411.
- (26) Hitchcock, A. P.; Beaulieu, S.; Steel, T.; Stohr, J.; Sette, F. *J. Chem. Phys.* **1984**, *80* (9), 3927.
- (27) Ito, K. *J. Electron Spectrosc. Relat. Phenom.* **2001**, *15*, 114.
- (28) Pavlychev, A. A.; Hallmeier, K. H.; Hennig, C.; Szargan, R. *Chem. Phys.* **1995**, *201*, 547.
- (29) Pedio, M.; Fuggle, J. C.; Somers, J.; Umbach, E.; Haase, J.; Lindner, Th.; Hofer, U.; Grioni, M.; de Groot, F. M. F.; Hillert, B.; Becker, L.; Robinson, A. *Phys. Rev. B* **1989**, *40*(11), 7924.
- (30) Wood, G. A.; Iroh, J. O. *Synth. Met.* **1996**, *80*, 73.
- (31) Mckeown, D. A. *J. Non-Cryst. Solids* **1994**, *180*(1), 1.
- (32) Ettegui, E.; Razafitrimo, H.; Gao, Y.; Hsieh, B. R.; Feld, W. A.; Ruckman, M. W. *Phys. Rev. Lett.* **1996**, *76*(2), 299. (b) Tourillon, G.; Guay, D.; Fontaine, A.; Garret, R.; Willians, G. P. *Faraday Discuss. Chem. Soc.* **1990**, *89*, 275.